RESEARCH ARTICLE | MARCH 21 2025

Diffraction in phase space: Jumps and kinks in matter waves revealed by their dynamics

Gregor Finkbeiner ; Maxim A. Efremov ; Robert F. O'Connell ; Wolfgang P. Schleich

Chaos 35, 033150 (2025)
https://doi.org/10.1063/5.0260470

Diffraction in phase space: Jumps and kinks in matter waves revealed by their dynamics

Cite as: Chaos 35, 033150 (2025); doi: 10.1063/5.0260470
Submitted: 24 January 2025 · Accepted: 3 March 2025 ·
Published Online: 21 March 2025

Gregor Finkbeiner,[1,a)] Maxim A. Efremov,[1,2,b)] Robert F. O'Connell,[3,c)] and Wolfgang P. Schleich[1,4,d)]

AFFILIATIONS

[1]Institut für Quantenphysik and Center for Integrated Quantum Science and Technology (IQST), Universtät Ulm, Albert-Einstein-Allee 11, D-89081 Ulm, Germany
[2]German Aerospace Center (DLR), Institute for Quantum Technologies, D-89081 Ulm, Germany
[3]Department of Physics and Astronomy, Louisiana State University, Baton Rouge, Louisiana 70803-4001, USA
[4]Institute for Quantum Science and Engineering (IQSE), Texas A&M AgriLIfe Research and Hagler Institute for Advanced Study, Texas A&M University, College Station, Texas 7784-4242, USA

[a)]**Author to whom correspondence should be addressed:** gregor.finkbeiner@uni-ulm.de
[b)]maxim.efremov@dlr.de
[c)]rfoc@lsu.edu
[d)]wolfgang.schleich@uni-ulm.de

ABSTRACT

We show that a discontinuity either in a wave function or its derivative, corresponding to a jump or a kink, causes ripples in Wigner phase space. In the free time evolution, these structures give rise to interference fringes in the probability density represented in spacetime.

The time-dependent Schrödinger equation describes the time evolution of a wave function, but how do we prepare the initial wave function? An experimental technique routinely employed in matter wave optics starts from an energy eigenfunction of a binding potential and then suddenly removes the potential. The so-prepared wave function may exhibit a discontinuity, which in the subsequent time evolution manifests itself in fringes in spacetime. This phenomenon of diffraction in phase space is not limited to quantum mechanics but constitutes an ear mark of wave physics.

I. INTRODUCTION

Analyzing a quantum phenomenon from different points of views often leads to deeper insights and new effects. Indeed, the various formulations of quantum mechanics, such as matrix mechanics à la Heisenberg,[1] wave mechanics à la Schrödinger,[2] or the path integral approach à la Feynman,[3] frequently produce complementary explanations. In the present article, we employ the Wigner phase space distribution function[4] to explain the appearance of interference fringes in the free time evolution of discontinuous wave functions.

A. Stationary waves in potentials with jumps and kinks

The sudden approximation is an important tool in quantum mechanics.[5] An instantaneous change of a potential does not alter the quantum state but strongly influences its subsequent dynamics.

This feature stands out most clearly for an energy eigenstate of the original potential, which is obviously no longer an eigenstate of the new potential and, therefore, has to be expanded into its stationary states. Applications of sudden transitions range from molecular physics, where the corresponding transition probability amplitudes carry the name Franck–Condon factors,[6] to nuclear physics,[7] or the photon statistics of a squeezed state.[8]

The box potential that is constant over a finite region of space jumps to an infinite value at the boundaries. The corresponding infinitely steep and infinitely tall walls create energy wave functions, which vanish outside of the box. As a result, the Franck–Condon factors of two displaced box potentials do not add up to unity.[9]

In order to resolve the mystery of the *missing probability*, we have considered[9] the transition probability amplitudes between energy eigenstates of two suddenly displaced irrigation canal potentials. In contrast to the box, the canal does not display jumps but kinks due to the finite steepness of the walls.

In this analysis, we have noticed[9] rapid oscillations in the tails beyond the upper Franck–Condon maximum. They result[9]

. . .from the interference of secondary WKB waves created by scattering the original waves off the sharp corners of the irrigation canal.

Kinks in a potential act[10] as sources of new waves modifying the energy wave functions and manifesting themselves in the rapid oscillations of the Franck–Condon factors. This effect is opposite to the goal of the stealth plane[11] to avoid reflections from corners.

B. Freely propagating waves with jumps and kinks

The phenomenon of sharp corners in a potential as the origin of secondary waves[10] represents one side of the coin. The manifestation of sharp corners, that is, kinks in wave functions rather than potentials, in fringes in spacetime constitutes the other side. We devote our present article to the analysis of this effect and, in particular, study the influence of jumps and kinks in the wave function on its subsequent free dynamics.[12,13]

The most familiar example is the scattering of a scalar wave from a sharp edge, that is, a half-plane giving rise to an intensity distribution in the far field governed by the Cornu spiral.[14] Starting from the domain of the shadow, the intensity increases and oscillates around a steady state in the bright regime. We show that these oscillations are indeed a consequence of fringes in spacetime caused by the jump of the wave function at the sharp edge.

Deeper insight into the scattering from a sharp edge springs from Wigner phase space.[15,16] Whereas the initial wave function prepared by the edge is constant and non-zero over the accessible half-line, the corresponding Wigner function displays oscillatory waves with positive and negative values. These ripples in phase space give rise to intensity variations in the far-field distribution due to the shearing effect of the initial Wigner function induced by the free time evolution.

Our interest in this problem stems from a much more involved analysis[17] of the dynamics of a neutron bouncing from a mirror in the linear gravitational potential of the Earth. In the so-called *q*Bounce,[18,19] the spacetime representation of the probability density displays prominent fringes[20] in the short time limit, reminiscent of quantum carpets.[21–23] In these investigations, the initial wave function was the displaced ground state of the linear potential with an infinitely steep and an infinitely tall wall. The ground state wave function of this potential vanishes underneath the wall, but increases linearly in the immediate neighborhood outside of the wall, creating a kink.

We emphasize that our analysis corresponds to a situation in which we suddenly remove not only the infinitely tall wall confining the particle but also the linear potential. In this case, the *q*Bounce wave function undergoes free time evolution.

However, in the *q*Bounce setup,[18] only the wall is removed and the linear potential remains. As a result, now, the wave function experiences the propagator of a particle in the presence of a constant force. Since in the short-time limit the two expressions will agree this elementary calculation provides a first insight into the fringes found in simulations of the *q*Bounce experiment.

An even more complicated situation arises when there is an additional infinitely tall wall down stream. In this case, the propagator is determined by all bound states. However, a discussion of this arrangement[17] goes beyond the scope of the present article.

In order to focus on the essentials of the creation of fringes in spacetime from jumps and kinks in wave functions, we employ three elementary models. To start with, we consider two examples of wave functions having a jump in their values. We then turn to one in the derivative. We conclude with the exact displaced ground state wave function of *q*Bounce. In all cases, we calculate the corresponding Wigner function and discuss its free time evolution.

C. Overview

Our article is organized as follows: in Sec. II, we consider the influence of the restriction of a particle to positive coordinates, on the Wigner function, and point out the associated phenomenon of diffraction in Wigner phase space.[15,16] We then identify ripples in the Wigner function originating from a discontinuity either in the wave function or its first derivative. For this purpose, we analyze in Sec. III the four wave functions and their corresponding Wigner functions: The Heaviside step function and the discontinuous exponential function display a jump in the wave function at the origin. In contrast, the modified exponential and the *q*Bounce wave functions are continuous at the origin but show a discontinuity in the first derivative. The ripples are most pronounced for the Heaviside step function.

We then demonstrate in Sec. IV that the ripples in Wigner phase space manifest themselves[23] in the free time evolution in fringes in spacetime. For the Heaviside function, the fringes are most prominent but softened for the other cases. We conclude in Sec. V by briefly summarizing our results and providing an outlook.

In order to keep the article self-contained, we have included several appendixes presenting detailed derivations. In Appendix A, we obtain an alternative expression for the Wigner function in terms of the diffraction kernel and verify that the Wigner function of the Heaviside step function satisfies this integral relation. We then perform in Appendix B the integration of the Wigner function for the modified exponential function and express in Appendix C the Wigner function of the *q*Bounce wave function in terms of an integral, which allows us to obtain a qualitative understanding of its behavior. Moreover, we prove that this Wigner function also obeys the diffraction integral equation derived in Appendix A. We dedicate Appendix D to the free time evolution of the Heaviside step function as well the exponential and the modified exponential functions. In Appendix E, we address the corresponding problem for the *q*Bounce wave function and find an integral representation convenient for a numerical evaluation.

II. DIFFRACTION IN THE WIGNER PHASE SPACE

In this section, we consider the Wigner function of a wave function that is non-vanishing for positive coordinates only. We show that this restriction of the particle to the positive half-line leads in

the definition of the Wigner function to a *finite* region of integration and, thus, to a diffraction in phase space. This feature stands out most clearly in an implicit expression for the Wigner function in the form of an integral equation with a diffraction kernel. Throughout the article, we consider the one-dimensional problem of a non-relativistic particle of mass m and coordinate z.

A. Finite integration in a Wigner function

For the sake of simplicity, we assume the discontinuity either in the wave function or its first derivative to be at the origin and study the wave function

$$\psi(z) \equiv \Theta(z)\,\varphi(z). \tag{1}$$

Here, Θ denotes the Heaviside step function, and the wave function $\varphi = \varphi(z)$ for positive coordinates is real.

To gain deeper insight into the influence of a discontinuity in the wave function, we recall the definition[15,16]

$$W_\psi(z,k) = \frac{1}{2\pi}\int_{-\infty}^{\infty} \mathrm{d}y\, \mathrm{e}^{iky}\psi^*\left(z+\frac{y}{2}\right)\psi\left(z-\frac{y}{2}\right) \tag{2}$$

of the Wigner function living in quantum phase space formed by the coordinate z and the wave vector k.

When we substitute Eq. (1) into Eq. (2), we find the expression

$$W_\psi(z,k) = \Theta(z)\, W_\varphi(z,k), \tag{3}$$

where

$$W_\varphi(z,k) \equiv \frac{1}{2\pi}\int_{-2z}^{2z} \mathrm{d}y\, \mathrm{e}^{iky}\varphi\left(z+\frac{y}{2}\right)\varphi\left(z-\frac{y}{2}\right). \tag{4}$$

Here, we have used the identity[24]

$$\Theta\left(z-\frac{y}{2}\right)\Theta\left(z+\frac{y}{2}\right) = \Theta(z)\,\Theta\left(|y|-2z\right) \tag{5}$$

and the fact that φ is real.

Hence, the restriction of the wave function ψ to positive values only, as described by Eq. (1), has three characteristic effects on the Wigner function W_ψ: (i) it is the product of a Heaviside function and the Wigner function of W_φ, (ii) for this reason, the phase space of W_ψ is restricted to the domain of positive coordinates only, and (iii) it replaces the *infinite* domain of integration by a *finite* one, given by the coordinate z.

Moreover, we note the symmetry relation

$$W_\psi(z,-k) = W_\psi(z,k), \tag{6}$$

which follows immediately from Eq. (4) upon replacing the integration variable y by $\bar{y} \equiv -y$. In the examples discussed in our article, this symmetry is apparent.

B. Diffraction kernel in the phase space

The finite region of integration in the Wigner function W_φ creates a sinc function familiar from diffraction phenomena.[14] This fact stands out most clearly in the examples discussed in Sec. III but also from the integral equation

$$W_\psi(z,k) = \Theta(z)\int_{-\infty}^{\infty} \mathrm{d}k'\, W_\psi(z,k')\mathcal{D}(2z,k+k'), \tag{7}$$

derived in Appendix A which contains the diffraction kernel

$$\mathcal{D}(a,u) \equiv \frac{1}{\pi}\frac{\sin(ua)}{u}, \tag{8}$$

as well as the Wigner function W_ψ.

Although, any Wigner function W_ψ, which corresponds to a wave function restricted to a half-line, must satisfy the integral equation, Eq. (7), this relation does not specify W_ψ uniquely. This feature is obvious since Eq. (7) is solely a consequence of the fact that ψ vanishes for negative values of z and does not contain any information about the form of the discontinuity, that is, either a jump in ψ or in its first derivative.

Nevertheless, Eq. (7) demonstrates that the finite region of integration in Eq. (4) defining the Wigner function W_φ creates a diffraction in phase space, expressed by the diffraction kernel $\mathcal{D}$, and contained in the convolution of W_ψ and $\mathcal{D}$. This convolution is only in the wave vector variable but not in the coordinate.

III. RIPPLES IN THE WIGNER PHASE SPACE

In Sec. II, we have shown that the restriction of the particle to positive coordinates only, leads in the Wigner function to the integration over a finite region of the coordinate analogous to the diffraction from a single slit.[14] In this section, we show that this phenomenon leads to ripples in Wigner phase space and illustrate them using four examples where the wave function either jumps or displays a kink.

A. Discontinuity in the wave function

We start our discussion with a wave function, which vanishes for negative coordinates but jumps at the origin either to a constant function or to an exponentially decaying function. In both cases, we obtain elementary analytical expressions for the corresponding Wigner functions.

1. Jump to a constant wave function

To identify the effect of the discontinuity of the wave function on the Wigner function most clearly, we set

$$\varphi_c(z) \equiv 1, \tag{9}$$

that is,

$$\psi_c(z) \equiv \Theta(z), \tag{10}$$

and Eq. (4) reduces to the expression

$$W_c(z,k) = \Theta(z)\,\frac{1}{\pi}\frac{\sin(2kz)}{k} = \mathcal{D}(2z,k), \tag{11}$$

shown in Fig. 1(a) and given by the diffraction kernel, Eq. (8).

Hence, at a given coordinate z, the Wigner function W_c is a sinc function in the wave vector k with a dominant maximum at $k = 0$ and a characteristic decay of $1/k$. It oscillates between positive

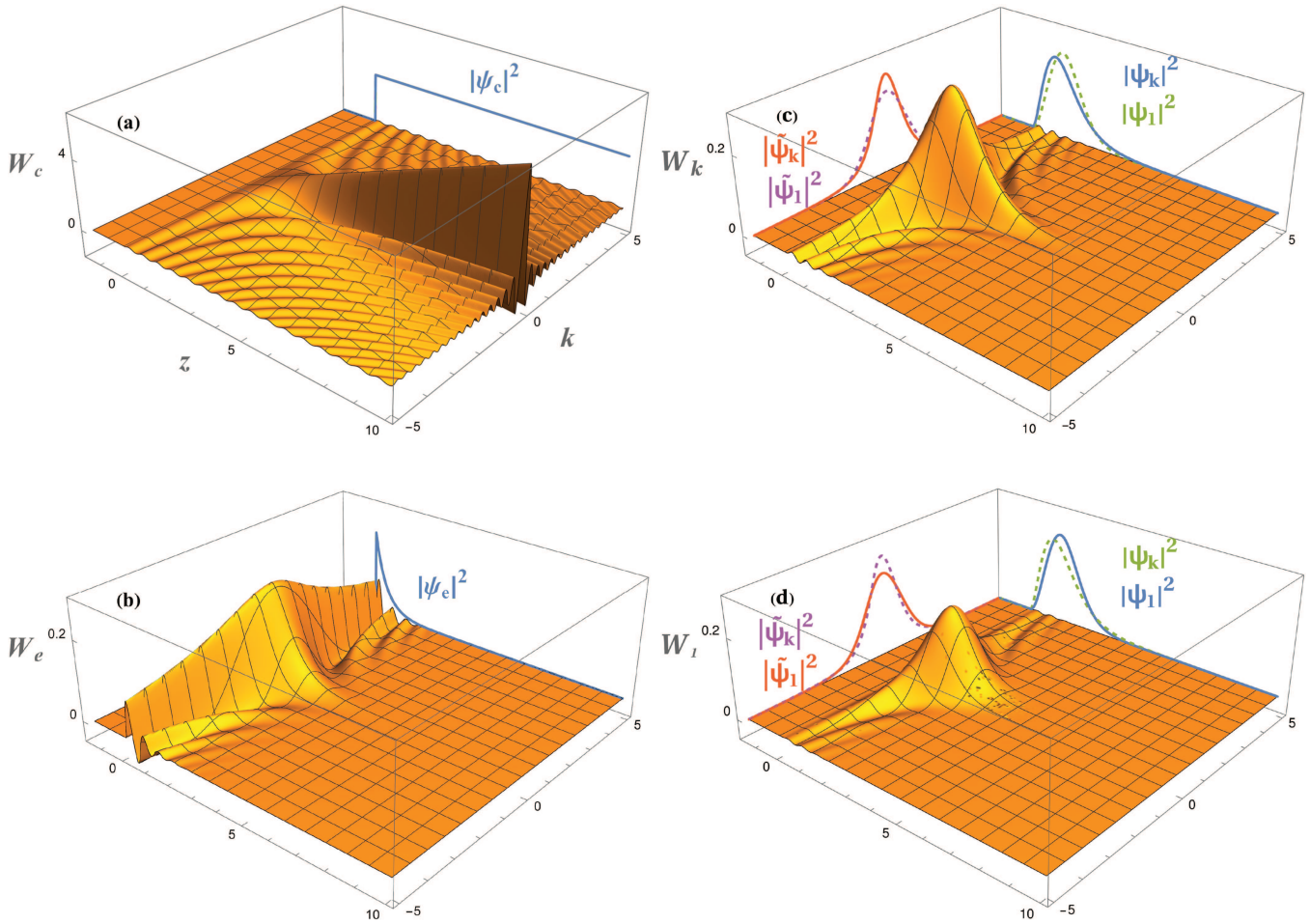

FIG. 1. Ripples in Wigner phase space caused by a jump (left column) in, or a kink (right column) of a wave function. In (a) and (b), we show the Wigner functions W_c and W_e resulting from the wave functions ψ_c and ψ_e with a discontinuity, and in (c) and (d), we display the resulting Wigner functions W_k and W_1 associated with the wave functions ψ_k and ψ_1 with a discontinuity in the first derivative. In the corresponding back drops, we depict the probability densities (not to scale) in position or wave vector space obtained by integrating the Wigner function over k or z. Since ψ_c is not normalizable, there does not exist a wave vector distribution in (a). The Wigner functions W_k and W_1 shown in (c) and (d) lead to similar probability densities shown by solid curves. The dashed curves in (c) and (d) correspond to the Wigner functions displayed in (d) and (c). Here, we have used the decay parameter $\beta = 1$.

and negative values, giving rise to the ripples in Wigner phase space apparent in Fig. 1(a).

These ripples are reminiscent of the waves caught in the bay formed by the inflection point of the classical trajectory corresponding to an energy eigenstate in a Morse potential.[25,26] They also appear in numerous Wigner functions of quantum systems, such as the hydrogen atom,[27,28] or closed shell atoms,[29] and manifest themselves in fringes decorating anticaustics.[30] In these examples, the waves can be understood with the help of the cord construction[31] as an interference in phase space. However, in the present case, there is no classical trajectory and, thus, no cord construction.

In the neighborhood of the positive z axis, W_c is positive and grows on the z axis linearly with z without a bond. This dominant behavior reflects the fact that ψ_c is not normalizable.

The negative parts of W_c contained in the ripples are necessary in order to satisfy the marginal property,

$$\int_{-\infty}^{\infty} \mathrm{d}k\, W_\psi(z,k) = |\psi(z)|^2\,, \tag{12}$$

valid for any square integrable function, which for W_c, given by Eq. (11), reads

$$\frac{\Theta(z)}{\pi} \int_{-\infty}^{\infty} \mathrm{d}k\, \frac{\sin(2kz)}{k} = \Theta(z) = |\psi_c(z)|^2\,. \tag{13}$$

Here, we have used the integral relation

$$\int_{-\infty}^{\infty} \mathrm{d}x\, \frac{\sin x}{x} = \pi \tag{14}$$

and the identity

$$\Theta^2 = \Theta. \tag{15}$$

In the backdrop of Fig. 1(a), we display the constant probability density $|\psi(z)|^2$, resulting from W_c by integration over k.

We note that there exists also the marginal property[15,16]

$$\int_{-\infty}^{\infty} \mathrm{d}z\, W_\psi(z,k) = |\tilde{\psi}(k)|^2, \tag{16}$$

where $\tilde{\psi} = \tilde{\psi}(k)$ denotes the Fourier transform of the wave function $\psi = \psi(z)$. Since ψ_c is not normalizable, this marginal property cannot lead to convergent results.

It is interesting that apart from the Heaviside function, the diffraction kernel $\mathcal{D}$ given by Eq. (8) and the Wigner function W_ψ in Eq. (11) are identical. Due to the convolution identity, Eq. (A15) of two diffraction kernels derived in Appendix A, W_ψ satisfies the diffraction integral, Eq. (7).

2. Jump to an exponential wave function

Obviously, the exponential wave function

$$\varphi_e(z) \equiv N_e \mathrm{e}^{-\beta z} \tag{17}$$

with the normalization constant

$$N_e \equiv \sqrt{2\beta}, \tag{18}$$

and the decay parameter β is normalizable.

In this case, the corresponding Wigner function W_e, for

$$\psi_e(z) \equiv \Theta(z)\, \varphi_e(z) \tag{19}$$

following from Eqs. (4) and (17), reads

$$W_e(z,k) = \Theta(z)\, \frac{N_e^2}{\pi} \mathrm{e}^{-2\beta z} \frac{\sin(2kz)}{k}. \tag{20}$$

Here, we have used the identity

$$\mathrm{e}^{-\beta(z+y/2)} \mathrm{e}^{-\beta(z-y/2)} = \mathrm{e}^{-2\beta z} \tag{21}$$

reducing the integral in Eq. (4) for the Wigner function to that of the constant wave function φ_c.

Hence, the only change is a position-dependent exponential term, combined with the normalization constant N_e^2. Both originate from the normalization of φ_e and multiply the Wigner function W_c corresponding to ψ_c leading us to the connection

$$W_e = N_e^2 \mathrm{e}^{-2\beta z} W_c. \tag{22}$$

The consequences of this change from a constant to an exponentially decaying wave function are clearly visible in Fig. 1(b). In the neighborhood of the positive z axis and for large values of z, W_e is governed by the exponential term in Eq. (20). For small values of z, the linear growth still dominates creating in this way a maximum where these two behaviors merge into each other.

The exponential prefactor in Eq. (22) has an additional effect. It reduces the amplitudes of the ripples, a feature that stands out most clearly in a comparison of Figs. 1(a) and 1(b).

We conclude our discussion of W_e by noting that it satisfies the diffraction integral equation, Eq. (7). At this point, it is important that the convolution is only in the variable k. For this reason, the product of a function that only depends on the coordinate, and W_c, which is a solution, is also a solution.

B. Discontinuity in the derivative

So far, we have discussed the influence of a discontinuity in the *wave function* on the corresponding Wigner function. We now address the analogous problem for a discontinuity in the *derivative* of a wave function and illustrate our results using two examples: (i) a decaying exponential function multiplied by the coordinate and (ii) an energy wave function[32,33] of a particle, such as an atom[34,35] or a neutron[36] moving in the Earth's gravitational field[37] in the presence of an infinitely tall and infinitely steep potential wall.

1. Kink in the modified exponential

For the sake of simplicity, we start our discussion with the modified exponential wave function,

$$\varphi_k(z) \equiv N_k z \mathrm{e}^{-\beta z} \tag{23}$$

with the normalization constant $N_k \equiv \sqrt{4\beta^3}$.

According to Appendix B, the Wigner function W_k associated with the wave function

$$\psi_k(z) \equiv \Theta(z)\, \varphi_k(z) \tag{24}$$

with a kink, following from Eq. (4), now reads

$$W_k(z,k) = \Theta(z)\, \frac{N_k^2}{2\pi} \mathrm{e}^{-2\beta z} \left[\frac{\sin(2kz)}{k^3} - 2z \frac{\cos(2kz)}{k^2} \right]. \tag{25}$$

When we compare this expression for W_k, to the one, Eq. (20), corresponding to the Wigner function W_e of a wave function with a jump, we find that W_k is still some sort of sinc function as a function of k, multiplied by the exponential decaying as a function of z. However, now the characteristic decay of W_k in k is governed by $1/k^2$ instead of $1/k$, as shown in Fig. 1(c). As a result, the ripples in phase space are slightly weaker than for a wave function with a jump.

2. Kink in qBounce wave functions

In the case of a quantum particle bouncing on a mirror in the Earth's gravitational field, the energy eigenfunctions are of the form of Eq. (1), and the Heaviside step function Θ results from the mirror placed at $z = 0$. Here, we assume that the particle cannot enter the surface of the mirror creating the condition $\psi(z) = 0$ for $z < 0$.

For $z > 0$, the energy wave functions[38]

$$\varphi_{\mathrm{n}}(z) \equiv N_{\mathrm{n}} \mathrm{Ai}(\kappa z - \epsilon_{\mathrm{n}}) \tag{26}$$

are given in terms of the Airy function[39] Ai, and the boundary condition at the mirror enforces the dimensionless energy $\epsilon_{\mathrm{n}} = -a_{\mathrm{n}}$ to be determined by the nth zero a_n of the Airy function with $\mathrm{Ai}(a_n) = 0$. The parameter

$$\kappa \equiv \left(\frac{2m^2 g}{\hbar^2} \right)^{1/3} \tag{27}$$

with the unit 1/length involves the acceleration g and makes the argument of Ai dimensionless, and the normalization constant[9]

$N_n \equiv \sqrt{\kappa}/|\mathrm{Ai}'(a_n)|$ contains the first derivative Ai' of the Airy function.

We now analyze manifestations of the kink in the eigenfunction,

$$\psi_n(z) \equiv \Theta(z)\,\varphi_n(z), \tag{28}$$

in the corresponding Wigner function W_n. For this purpose, we substitute φ_n given by Eq. (26) into the expression, Eq. (4), for the Wigner function. Unfortunately, to the best of our knowledge, there does not seem to be an analytical expression for this integral.

Nevertheless, we can gain some insight into the behavior of W_n when we cast in Appendix C this integral into the form

$$W_n(z,k) = \Theta(z)\,2^{1/3}\frac{N_n^2}{\pi^2}\int_{-\infty}^{\infty} \mathrm{d}u\,\mathrm{Ai}[u^2 + 2^{2/3}(\kappa z - \epsilon_n)] \times \mathcal{D}\left(2z, k - 2^{2/3}u\right), \tag{29}$$

which contains explicitly the diffraction kernel $\mathcal{D}$ given by Eq. (8). It is, therefore, not surprising that W_n satisfies the diffraction equation, Eq. (7), as also shown in Appendix C

In Fig. 1(d), we depict the numerically evaluated W_1, which displays features reminiscent of the examples discussed earlier. In particular, we recognize again the ripples in phase space, however, with a stronger damping than before.

IV. FRINGES IN SPACETIME

We now turn our attention to the dynamics of wave functions with a discontinuity and show that ripples in Wigner phase space lead to fringes in spacetime. In particular, we study the free time evolution of a wave function, Eq. (1), which enjoys non-vanishing values for positive coordinates only. Here, we employ two different tools: (i) the propagator of the wave function of a free particle given[3] by a quadratic phase factor and (ii) the propagator of the Wigner function consisting[15,16] of the product of two delta function in z and k, ensuring propagation along classical trajectories.

A. Fresnel transform vs shearing

For this purpose, we first recall[3] the propagator

$$G_\psi(z,t|z_0) \equiv N_p(t)\mathrm{e}^{i\alpha(t)(z-z_0)^2} \tag{30}$$

of a free particle with the normalization constant

$$N_p(t) \equiv \sqrt{\frac{\alpha(t)}{i\pi}} \tag{31}$$

and the abbreviation

$$\alpha(t) \equiv \frac{m}{2\hbar t}. \tag{32}$$

Hence, the Huygens integral determining the propagated wave function

$$\psi(z,t) = \int_{-\infty}^{\infty} \mathrm{d}z_0\, G_\psi(z,t|z_0)\psi(z_0) \tag{33}$$

reduces for wave functions of the type of Eq. (1) to the expression

$$\psi(z,t) = N_p(t)\int_0^{\infty} \mathrm{d}z_0\, \mathrm{e}^{i\alpha(t)(z-z_0)^2}\varphi(z_0). \tag{34}$$

It is interesting to compare and contrast the propagation of the wave function ψ, given by Eq. (33), in terms of the rather opaque Fresnel transform, with the propagation[15,16]

$$W(z,k;t) = \int_{-\infty}^{\infty}\mathrm{d}z_0\int_{-\infty}^{\infty}\mathrm{d}k_0\, G_W(z,k,t|z_0,k_0)\,W_0(z_0,k_0) \tag{35}$$

of the initial Wigner function $W_0(z,k) \equiv W(z,k;t=0)$ along the classical trajectories expressed by the propagator

$$G_W(z,k,t|z_0,k_0) \equiv \delta\left[z - \left(z_0 + \frac{\hbar k}{m}t\right)\right]\delta\left(k - k_0\right). \tag{36}$$

Indeed, the first delta function ensures that a particle reaches the coordinate z only along the Newton trajectory starting at $t = 0$ at z_0. The second delta function reflects conservation of momentum $\hbar k$ as required by free motion.

When we use the two delta functions to perform the integration in Eq. (35), we arrive at the expression

$$W(z,k;t) \equiv W_0\left(z - \frac{\hbar k}{m}t, k\right) \tag{37}$$

corresponding to a shearing of the initial Wigner function W_0.

Obviously, points in phase space with larger k move faster compared to ones with smaller k and, therefore, move further during the time t. Points on the coordinate axis, corresponding to $k = 0$, remain at rest.

B. From ripples to fringes

So far, we have considered the time evolution of an arbitrary initial state in the frameworks of the Schrödinger wave function and the Wigner function. We now apply these results to the four examples discussed in Sec. III. For details of the integration, we refer to Appendixes D and E.

1. Scattering from a sharp edge: Constant wave

The problem of the propagation of a constant wave function, which jumps at the origin from a vanishing value to a non-vanishing one, such as the wave function ψ_c Eq. (10), corresponds to scattering a scalar wave off a sharp edge.[14] In this case, Eq. (34) reduces to the expression

$$\psi_c(z,t) = \frac{1}{2}\mathrm{erfc}\left[-\sqrt{\frac{\alpha(t)}{i}}z\right] \tag{38}$$

in terms of the complementary error function[40] erfc as verified in Appendix D.

In Fig. 2(a), we display the probability density $|\psi_c|^2$ in time and space, and fringes in spacetime emerge from the origin. They are a consequence of the ripples in the Wigner function, which experience a shearing due to the free time evolution.

In order to bring this fact out most clearly, we show in Fig. 3 the time evolution of the Wigner function W_c of the constant wave function ψ_c given by Eq. (11) for four typical times. Here, we use a two-dimensional representation of W_c rather than the three-dimensional one of Fig. 1 to better highlight the influence of the phase space ripples. Indeed, positive and negative values of W_c are indicated by bright or dark colors.

According to Eq. (37), the propagation of W_c due to free motion leads to a shearing of the initial Wigner function. As a result,

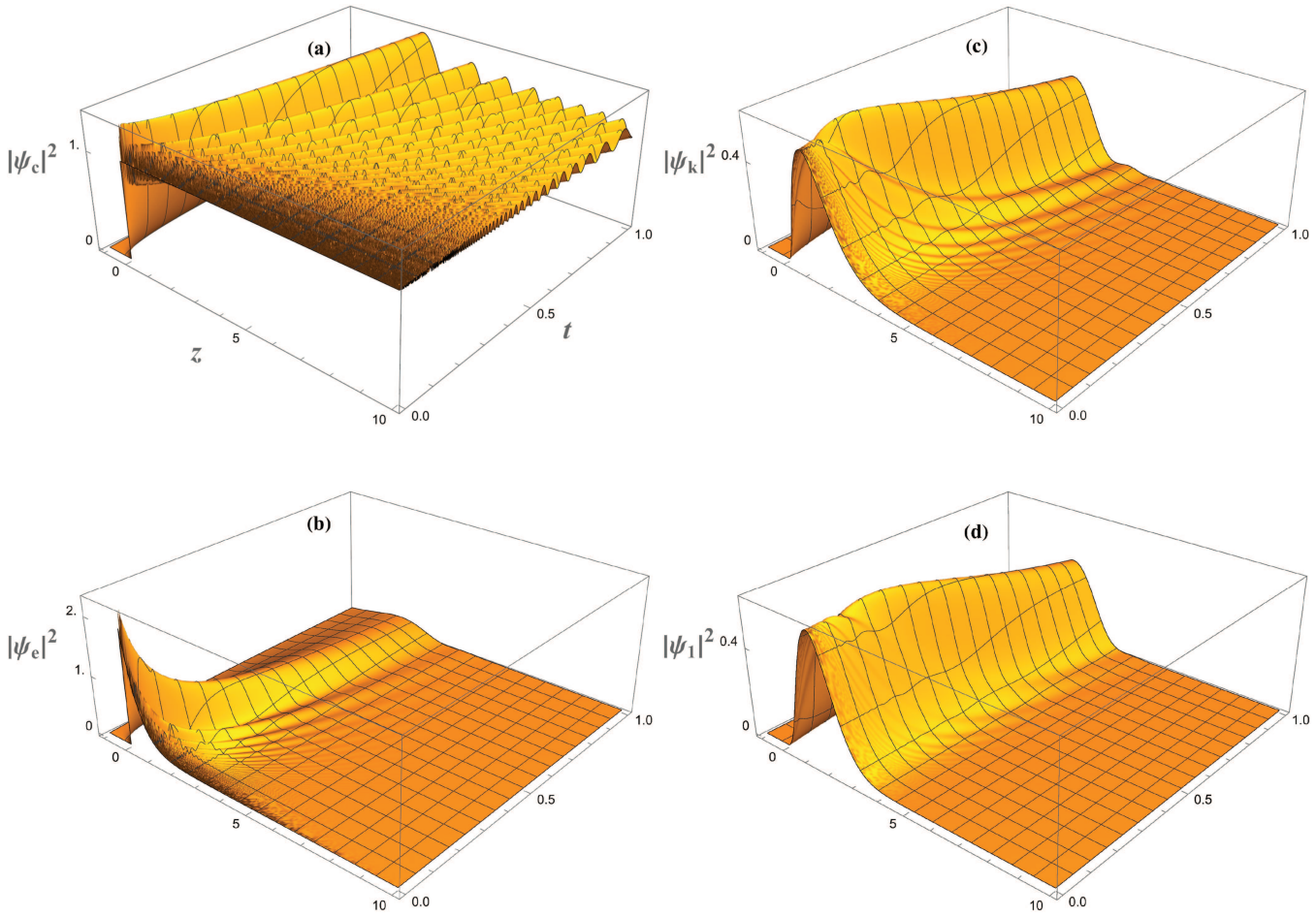

FIG. 2. Fringes in spacetime caused by a jump (left column) in or a kink (right column) of a wave function. In (a) and (b), we show the probability density in spacetime resulting from the free propagation of the initial wave functions ψ_c and ψ_e, whereas in (c) and (d), we depict the same phenomenon for ψ_k and ψ_1. In the course of time, the sharp edge in (a) at $z = 0$ moves to the right while developing ever more sidelobes. This phenomenon is less pronounced in the three other examples due to the fact that the fringes are not carved into a constant background as in (a), but appear in the tails of the original maximum, which is slowly decaying while spreading. However, we emphasize that in the short-time limit, the wave packets ψ_k and ψ_1, depicted in (c) and (d), briefly focus as apparent from the temporary increase of the central maximum. Here, we have used the decay parameter $\beta = 1$.

the ripples move to the right or left depending on the sign of k. Since they appear for non-vanishing values of k, they move faster than the dominant maximum along the z axis and, thus, modulate this background, which leads to fringes in the probability density when integrated over k as expressed by the marginal property, Eq. (13). The long-time limit yields the familiar probability density governed by the Cornu spiral.[14]

2. Scattering from a sharp edge: Decaying wave

Next, we turn to the time evolution of the wave function ψ_e defined by Eq. (17) and find according to Appendix D the expression

$$\psi_e(z,t) = \sqrt{\frac{\beta}{2}} e^{-\beta z} e^{\frac{i\beta^2}{4\alpha(t)}} \operatorname{erfc}[b(z,t)], \tag{39}$$

with the abbreviation

$$b(z,t) \equiv -\sqrt{\frac{\alpha(t)}{i}} \left[z + \frac{\beta}{2i\alpha(t)} \right]. \tag{40}$$

In Fig. 2(b), we display the resulting probability density $|\psi_e|^2$ in time and space. Again, we find fringes in spacetime. However, in contrast to the corresponding distribution of ψ_c, they are not as pronounced. The reason for this behavior is the reduced amplitude of the ripples of the corresponding Wigner function W_e.

3. Scattering from a soft edge due to apodization

Since the wave function ψ_k is continuous at $z = 0$, we can interpret the subsequent time evolution as the result of the scattering of a scalar wave off a *soft* edge, that is, one with apodization. In

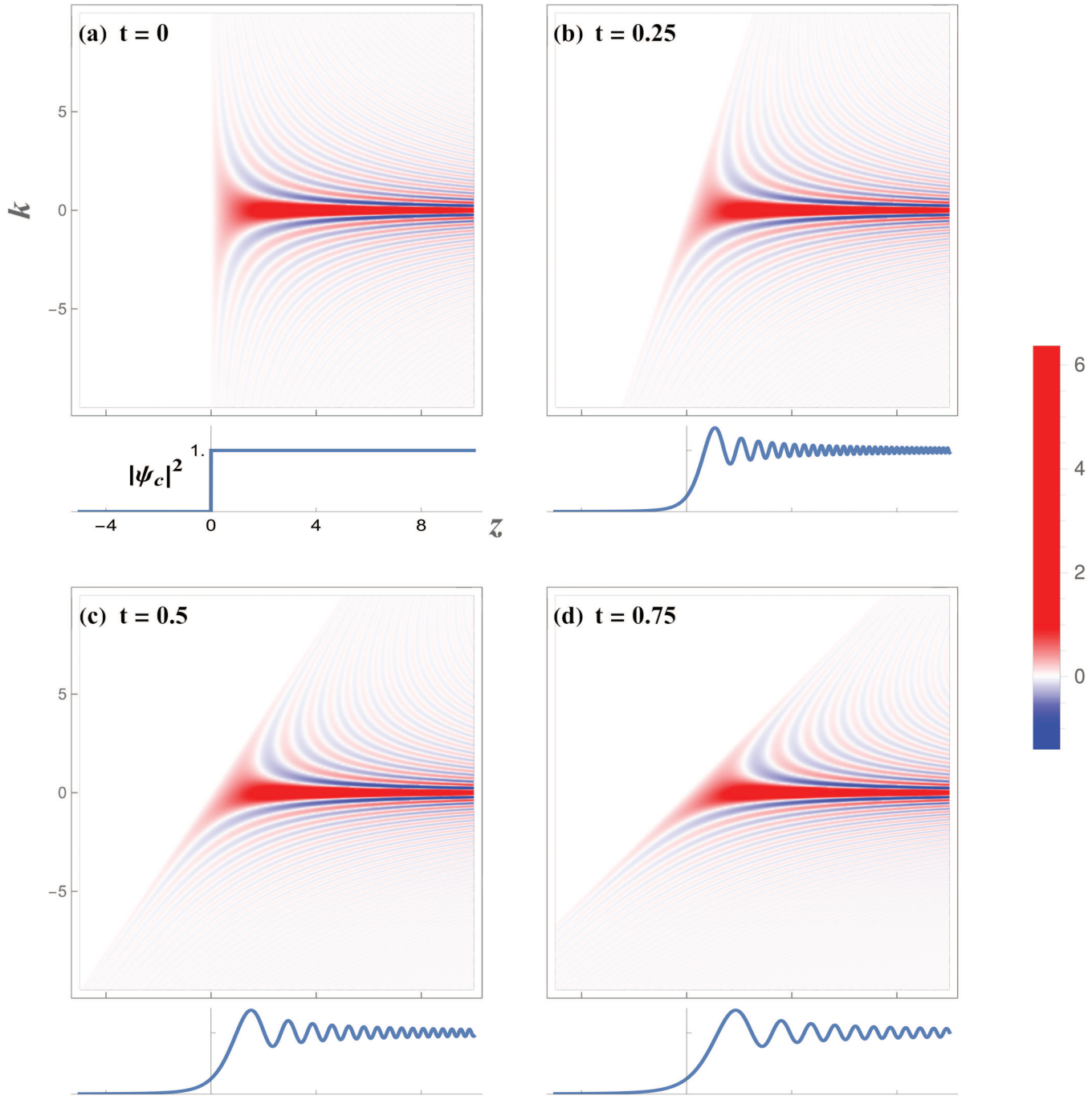

FIG. 3. From ripples in Wigner phase space to fringes in spacetime illustrated by the free time evolution of the Wigner function W_c corresponding to the wave function ψ_c, depicted here at four characteristic times. The free motion causes a shearing in phase space of the initial Wigner function represented by color plots. Bright and dark colors indicate positive and negative values of the function as suggested by the scale on the right. In the course of time, the ripples of the initial Wigner function of Fig. 1(a) get pushed more and more to the right for positive k, and to the left for negative k, and due to their oscillatory behavior alternating between positive and negative values create fringes in the tails of the probability density obtained by integrating over k. The scaling gs of the two orthogonal axes defining Wigner phase space is identical in the four pictures.

Appendix D, we then perform the Huygens integral for ψ_k and find

$$\psi_k(z,t) = \frac{N_k}{2} e^{-\beta z} e^{\frac{i\beta^2}{4\alpha(t)}} \sqrt{\frac{1}{\alpha(t)}} e^{i\frac{\pi}{4}} \times \left\{ b(z,t)\mathrm{erfc}[b(z,t)] - \frac{e^{-b(z,t)^2}}{\sqrt{\pi}} \right\}. \tag{41}$$

The probability density $|\psi_k|^2$ shown in Fig. 2(c) displays three characteristic features: (i) the appearance of fringes throughout spacetime originating at the starting position of the wave packet, (ii) the maximum of the wave packet is not at the origin of space and time, and (iii) there seems to be a focusing effect[41] of the wave packet for $t > 0$.

4. qBounce wave function

Finally, in Appendix E, we perform the Huygens integral for the *q*Bounce wave function, Eq. (26), and find

$$\psi_n(z,t) = \frac{N_n}{4\pi} \int_{-\infty}^{\infty} \mathrm{d}y\, \mathrm{erfc}\left\{ \sqrt{\frac{\alpha(t)}{i}} \left[\frac{y}{2\alpha(t)} - z \right] \right\} \times \exp\left\{ i \left[\frac{1}{3}y^3 - \frac{\kappa^2}{4\alpha(t)}y^2 + (\kappa z - \epsilon_n)y \right] \right\}. \tag{42}$$

In Fig. 2(d), we depict the numerically evaluated ground state probability density $|\psi_1(z,t)|^2$, which displays the same characteristic features as $|\psi_k|^2$ in Fig. 2(c), but with a dampened amplitude.

V. CONCLUSIONS

How does a discontinuity in the wave function, or in its first derivative, manifest itself in the free time evolution? In the present paper, we have addressed this question with the help of the Wigner function.

For this purpose, we have studied the time evolution of a free particle prepared initially in four different states corresponding to four different wave functions in position space: The Heaviside step function and the exponential display a jump in the wave function at the origin. The modified exponential and the *q*Bounce wave function show a discontinuity in the first derivative.

The choice of the first three examples is motivated by the fact that these wave functions enjoy Wigner functions determined by analytic expressions. Although we could not find an analytic expression for the Wigner function of the *q*Bounce wave function, we could still derive an integral representation, which allowed us to gain insight into this function. The unifying property of the Wigner functions discussed in this article is ripples in phase space. Here, the Wigner functions oscillate between positive and negative values.

The free time evolution of the Wigner function is given by a shearing of the initial distribution, and the ripples translate into fringes in spacetime. They are most pronounced in the case of the Heaviside step function. However, they also appear in the case of the *q*Bounce function but are less visible. In this way, the fringes in spacetime are generalizations of the oscillations in the far-field distribution of the scattering from a sharp edge.

We expect these ripple-induced fringes not only to appear in the free time evolution, but also in the presence of a linear potential as provided, for example, by a constant gravitational field. The *q*Bounce system would be the perfect setup to observe the discontinuity fringes of spacetime.

DEDICATION

We dedicate this article to the memory of our friend Jason Alfredo C. Gallas, an extremely innovative scientist, a dedicated teacher, and a wonderful human being. The hydrogen atom in external fields, granular dynamics, cancer models, and "shrimps" represent only a few of the numerous fields where Jason has left his mark. Two of us (R.F.O'C. and W.P.S.) have had the pleasure to have known him for over 40 years and the great fortune to have collaborated with him on different topics. We fondly remember our frequent visits to the library of the Max-Planck-Institute for Plasma Physics after lunch, browsing through the latest journals and searching for interesting developments. After his graduation from the University of Munich and his return to Brazil, our paths did not cross as often as they should have. For this reason, we were all looking forward to a reunion at a workshop in Baton Rouge in October 2023. Unfortunately, it had to take place without Jason, another manifestation of the old German proverb: "Der Mensch denkt und Gott lenkt."

ACKNOWLEDGMENTS

We thank H. Abele for bringing the appearance of the fringes in the early-time evolution of the *qBounce* experiment to our attention and for many illuminating discussions on this topic. Moreover, we are grateful to the anonymous referees for their suggestions, in particular, the use of the method of stationary phase. W.P.S. thanks the Texas A&M University for a Faculty Fellowship at the Hagler Institute for Advanced Study and to Texas A&M AgriLife for the support of this work.

AUTHOR DECLARATIONS

Conflict of Interest

The authors have no conflicts to disclose.

Author Contributions

Gregor Finkbeiner: Formal analysis (equal); Investigation (equal); Methodology (equal); Visualization (lead); Writing – original draft (lead); Writing – review & editing (equal). **Maxim A. Efremov:** Formal analysis (equal); Investigation (equal); Writing – review & editing (equal). **Robert F. O'Connell:** Investigation (equal); Validation (equal); Writing – review & editing (equal). **Wolfgang P. Schleich:** Conceptualization (lead); Formal analysis (equal); Investigation (equal); Methodology (equal); Supervision (lead); Writing – original draft (equal); Writing – review & editing (equal).

DATA AVAILABILITY

Data sharing is not applicable to this article as no new data were created or analyzed in this study.

APPENDIX A: WIGNER FUNCTION WITH A DIFFRACTION KERNEL

In this appendix, we perform the integration over the finite domain of the coordinate in the definition, Eq. (4), of the Wigner function with the help of the Fourier transform of the wave function. This analysis brings to light the diffraction kernel.

Indeed, we find an implicit equation for the Wigner function as a solution of an integral equation. The Wigner function of a wave function restricted to a half-line is a convolution of the Wigner function with the diffraction kernel. We first derive this equation and then illustrate it using the example of the Wigner function W_c corresponding to the wave function ψ_c with a jump to a constant value at $z = 0$.

1. Integral equation

We start our derivation by recalling the identity

$$\Theta^2(z) = \Theta(z) \tag{A1}$$

for the Heaviside step function Θ, which allows us to express the wave function ψ, given by Eq. (1), in the rather unusual form,

$$\psi(z) = \Theta(z)\,\psi(z). \tag{A2}$$

When we substitute this expression into the definition, Eq. (2), of the Wigner function, we can use the property, Eq. (5), of Θ to create finite limits in the integration over y but still keep ψ rather than φ in the integrand, leading us to the expression

$$W_\psi(z,k) = \frac{\Theta(z)}{2\pi}\int_{-2z}^{2z} \mathrm{d}y\, \mathrm{e}^{iky}\psi^*\left(z+\frac{y}{2}\right)\psi\left(z-\frac{y}{2}\right). \tag{A3}$$

When we compare this representation of W_ψ to the one of Eq. (4), the wave function ψ rather than φ appears in the integrand. Needless to say, Eqs. (A3) and (4) are identical due to the identity, Eq. (A1), of the Heaviside step function.

However, the appearance of ψ now allows us to employ the Fourier transform,

$$\tilde\psi(k) \equiv \frac{1}{\sqrt{2\pi}}\int_{-\infty}^{\infty} \mathrm{d}z\, \mathrm{e}^{ikz}\psi(z), \tag{A4}$$

of ψ with its inverse

$$\psi(z) \equiv \frac{1}{\sqrt{2\pi}}\int_{-\infty}^{\infty} \mathrm{d}k\, \mathrm{e}^{-ikz}\tilde\psi(k). \tag{A5}$$

For the one-sided wave function, Eq. (1), we find

$$\tilde\psi(k) = \frac{1}{\sqrt{2\pi}}\int_{0}^{\infty} \mathrm{d}z\, \mathrm{e}^{ikz}\varphi(z), \tag{A6}$$

and its inverse given by Eq. (A5) reads

$$\psi(z) \equiv \int_0^\infty \mathrm{d}z'\,\delta(z-z')\varphi(z'). \tag{A7}$$

The integration of the delta function over positive coordinates only creates the Heaviside step function, in complete agreement with Eq. (1).

Next, we substitute the representation, Eq. (A5), of ψ into Eq. (A3), and arrive at the expression

$$W_\psi = \frac{\Theta}{2\pi}\int_{-\infty}^{\infty}\mathrm{d}k_1\int_{-\infty}^{\infty}\mathrm{d}k_2\,\mathrm{e}^{i(k_1-k_2)z}\tilde\psi^*(k_1)\,\tilde\psi(k_2) \times \frac{1}{2\pi}\int_{-2z}^{2z}\mathrm{d}y\exp\left\{i\left[k+\frac{1}{2}(k_1+k_2)\right]y\right\}, \tag{A8}$$

which after performing the integration over y leads us to the representation

$$W_\psi = \frac{\Theta}{2\pi}\int_{-\infty}^{\infty}\mathrm{d}k_1\int_{-\infty}^{\infty}\mathrm{d}k_2\,\mathrm{e}^{i(k_1-k_2)z}\tilde\psi^*(k_1)\,\tilde\psi(k_2) \times \mathcal{D}\left[2z, k+\frac{1}{2}(k_1+k_2)\right], \tag{A9}$$

where we have introduced the diffraction kernel

$$\mathcal{D}(a,u) \equiv \frac{1}{2\pi}\int_{-a}^{a}\mathrm{d}y\,\mathrm{e}^{iuy} = \frac{1}{\pi}\frac{\sin(ua)}{u}. \tag{A10}$$

It is useful to introduce the new integration variables,

$$k_-\equiv k_1 - k_2 \qquad k_+\equiv\frac{1}{2}(k_1+k_2), \tag{A11}$$

resulting in

$$W_\psi = \Theta\int_{-\infty}^{\infty}\mathrm{d}k_+\,\tilde W_\psi(z,k_+)\mathcal{D}(2z,k+k_+), \tag{A12}$$

where we have introduced the abbreviation

$$\tilde W_\psi(z,k) \equiv \frac{1}{2\pi}\int_{-\infty}^{\infty}\mathrm{d}k_-\,\mathrm{e}^{ik_-z}\tilde\psi^*\left(k+\frac{k_-}{2}\right)\tilde\psi\left(k-\frac{k_-}{2}\right), \tag{A13}$$

which is the definition of the Wigner function in the wave vector space defined by Eq. (A4).

Since $\tilde W_\psi = W_\psi$, we arrive at the implicit equation

$$W_\psi(z,k) = \Theta(z)\int_{-\infty}^{\infty}\mathrm{d}k'\,W_\psi(z,k')\mathcal{D}(2z,k+k') \tag{A14}$$

for the Wigner function W_ψ. Indeed, W_ψ appears on both sides of the equation but gets integrated over the wave vector k' with the diffraction kernel $\mathcal{D}$ on the right-hand side.

2. Convolution of two diffraction kernels

At the very heart of the phenomenon of diffraction in phase space is the integral relation

$$\int_{-\infty}^{\infty}\mathrm{d}k_+\,\mathcal{D}(a,k_+)\mathcal{D}(a,k+k_+) = \mathcal{D}(a,k), \tag{A15}$$

which demonstrates that the diffraction kernel $\mathcal{D}$ given by Eq. (A10) is an eigenfunction of the diffraction integral.

It is interesting that the identity, Eq. (A15), is also central to numerical methods based on sinc functions.[42] Although it has been discussed extensively in this context, we now rederive it for the sake of completeness.

For this purpose, we substitute the definition, Eq. (A10), of $\mathcal{D}$ into the left-hand side of Eq. (A15) and evaluate the integral

$$I_c \equiv \frac{1}{\pi^2}\int_{-\infty}^{\infty} dk_+ \frac{\sin(k_+a)}{k_+}\frac{\sin[(k+k_+)a]}{k+k_+}. \tag{A16}$$

With the identities

$$\frac{1}{k_+}\frac{1}{k+k_+} = \frac{1}{k}\left[\frac{1}{k_+} - \frac{1}{k+k_+}\right] \tag{A17}$$

and

$$\sin[(k+k_+)a] = \sin(ka)\cos(k_+a) + \cos(ka)\sin(k_+a) \tag{A18}$$

together with

$$\sin(k_+a) = \sin[-ka + (k+k_+)a], \tag{A19}$$

or

$$\sin(k_+a) = -\sin(ka)\cos[(k+k_+)a] + \cos(ka)\sin[(k+k_+)a], \tag{A20}$$

we arrive at the representation

$$I_c = \frac{1}{\pi}\frac{\sin(ka)}{k}I_s + \frac{1}{\pi}\frac{\cos(ka)}{k}I_a \tag{A21}$$

of the integral I_c where we have introduced the abbreviations

$$I_s \equiv \frac{1}{\pi}\int_{-\infty}^{\infty} dk_+ \left\{\frac{\sin(2k_+a)}{2k_+} + \frac{\sin[2(k+k_+)a]}{2(k+k_+)}\right\} \tag{A22}$$

and

$$I_a \equiv \frac{1}{\pi}\int_{-\infty}^{\infty} dk_+ \left\{\frac{\sin^2(k_+a)}{k_+} + \frac{\sin^2[(k+k_+)a]}{k+k_+}\right\}. \tag{A23}$$

The integral I_a vanishes since the integrand is antisymmetric in the integration variable k_+, and with the integral relation

$$\int_{-\infty}^{\infty} dx \frac{\sin x}{x} = \pi, \tag{A24}$$

we arrive at

$$I_s = 1, \tag{A25}$$

and, thus, at

$$I_c = \frac{1}{\pi}\frac{\sin(ka)}{k}, \tag{A26}$$

which yields with the definition, Eq. (A10), of $\mathcal{D}$ the identity, Eq. (A15).

APPENDIX B: WIGNER FUNCTION OF THE MODIFIED EXPONENTIAL

In this appendix, we evaluate explicitly the Wigner function W_k of the modified exponential wave function,

$$\varphi_k(z) = -N_k\frac{\partial}{\partial\beta}\left(e^{-\beta z}\right), \tag{B1}$$

given by Eq. (23). Here, we have already replaced the linear argument z by the derivative with respect to the decay parameter β, which simplifies the integration in Eq. (4) over y.

Indeed, when we substitute Eq. (B1) into the definition, Eq. (4), of W_φ, we can factor the differentiations with respect to β_1, and β_2 out of the integral, and find the expression

$$W_\varphi = \frac{N_k^2}{2\pi}\frac{\partial^2}{\partial\beta_1\partial\beta_2}\left\{e^{-(\beta_1+\beta_2)z}\int_{-2z}^{2z} dy\, e^{\left[ik-\frac{1}{2}(\beta_1-\beta_2)\right]y}\right\}\Bigg|_{\beta_1=\beta_2=\beta}. \tag{B2}$$

Here, we first differentiate with respect to the two parameters and then set them equal, as indicated by the vertical line at the end of the equation.

The integral immediately leads us to the formula

$$W_\varphi = \frac{N_k^2}{2\pi}\frac{\partial^2}{\partial\beta_1\partial\beta_2}\left[\frac{e^{-2\beta_1 z}e^{2ikz} - e^{-2\beta_2 z}e^{-2ikz}}{ik - \frac{1}{2}(\beta_1-\beta_2)}\right]\Bigg|_{\beta_1=\beta_2=\beta}, \tag{B3}$$

which after the differentiation with respect to β_2 and β_1 yields the expressions

$$\begin{aligned} W_\varphi = \frac{N_k^2}{2\pi}\frac{\partial}{\partial\beta_1}\Bigg\{&\frac{-1}{\left[ik-\frac{1}{2}(\beta_1-\beta_2)\right]^2}\\ &\times\frac{1}{2}\left[e^{-2\beta_1 z}e^{2ikz} - e^{-2\beta_2 z}e^{-2ikz}\right]\\ &+\frac{1}{ik-\frac{1}{2}(\beta_1-\beta_2)}\left(-e^{-2\beta_2 z}e^{-2ikz}\right)(-2z)\Bigg\}\Bigg|_{\beta_1=\beta_2=\beta} \end{aligned} \tag{B4}$$

and

$$\begin{aligned} W_\varphi = \frac{N_k^2}{2\pi}\Bigg[&\frac{(-1)(-2)}{(ik)^3}\left(-\frac{1}{2}\right)\left(\frac{1}{2}\right)e^{-2\beta z}2i\sin(2kz)\\ &+\frac{1}{2}\frac{(-1)}{(ik)^2}(-2z)e^{-2\beta z}e^{2ikz}\\ &+\frac{(-1)(-2z)}{(ik)^2}\left(-\frac{1}{2}\right)\left(-e^{-2\beta z}e^{-2ikz}\right)\Bigg]. \end{aligned} \tag{B5}$$

Here, we have already set $\beta_1 = \beta_2 = \beta$ but have not combined yet all the factors as to keep track of their origins.

After minor algebra, we arrive at

$$W_\varphi = \frac{N_k^2}{2\pi}e^{-2\beta z}\left[\frac{\sin(2kz)}{k^3} - 2z\frac{\cos(2kz)}{k^2}\right]. \tag{B6}$$

Needless to say, we could have also found this formula by performing directly the integral, Eq. (4), defining the Wigner function W_φ, without introducing the two differentiations. However, in this case, the quadratic contribution in y arising from the linear dependence of φ_e, which is from the identity

$$\left(z+\frac{y}{2}\right)\left(z-\frac{y}{2}\right) = z^2 - \frac{1}{4}y^2, \tag{B7}$$

can also be evaluated by a second derivative with respect to β. It is interesting to note that in this approach, it is *not* a differentiation with respect to β_1 *and* β_2 but twice with respect to β.

APPENDIX C: WIGNER FUNCTION OF THE *q*BOUNCE WAVE FUNCTION

The Wigner functions W_n of the *q*Bounce energy eigenfunctions ψ_n given by Eq. (28) have been previously analyzed[37] by numerically integrating the corresponding integral following from the definition, Eq. (4), of the Wigner function. In the present Appendix, we cast this integral into a form, which makes it easy to read off the qualitative features of W_n. Moreover, we verify that W_n satisfies the diffraction integral equation.

1. Alternative representation

When we substitute the wave function, Eq. (28), into the definition, Eq. (4), of the Wigner function and introduce the new integration variable $\xi \equiv \kappa y/2$, we arrive at the expression

$$W_n(z,k) = \frac{\Theta(z)}{\kappa\pi} N_n^2 \, I\left(\kappa z - \epsilon_n, \frac{k}{\kappa}; \kappa z\right) \tag{C1}$$

with the integral

$$I(\zeta, p; a) \equiv \int_{-a}^{a} \mathrm{d}\xi \, \mathrm{e}^{i2p\xi} \mathrm{Ai}(\zeta + \xi)\mathrm{Ai}(\zeta - \xi), \tag{C2}$$

which with the help of the definition[39]

$$\mathrm{Ai}(x) = \frac{1}{2\pi} \int_{-\infty}^{\infty} \mathrm{d}t \, \exp\left[i\left(\frac{1}{3}t^3 + xt\right)\right] \tag{C3}$$

of the Airy function takes the form

$$I = \frac{1}{4\pi^2} \int_{-a}^{a} \mathrm{d}\xi \int_{-\infty}^{\infty} \mathrm{d}t_1 \int_{-\infty}^{\infty} \mathrm{d}t_2 \, \mathrm{e}^{i(2p + t_1 - t_2)\xi} \times \exp\left\{i\left[\frac{t_1^3 + t_2^3}{3} + \zeta(t_1 + t_2)\right]\right\}. \tag{C4}$$

Next, we interchange the integration over ξ with the ones over t_1 and t_2 and obtain

$$I = \frac{1}{2\pi^2} \int_{-\infty}^{\infty} \mathrm{d}t_1 \int_{-\infty}^{\infty} \mathrm{d}t_2 \, \exp\left\{i\left[\frac{t_1^3 + t_2^3}{3} + \zeta(t_1 + t_2)\right]\right\} \times \frac{\sin\left[(2p + t_1 - t_2)a\right]}{2p + t_1 - t_2}, \tag{C5}$$

which with the substitutions

$$t_- \equiv t_1 - t_2 \qquad t_+ \equiv \frac{1}{2}(t_1 + t_2), \tag{C6}$$

that is,

$$t_1 \equiv t_+ + \frac{1}{2}t_- \quad t_2 \equiv t_+ - \frac{1}{2}t_-, \tag{C7}$$

and the identity

$$\frac{t_1^3 + t_2^3}{3} = \frac{2}{3}t_+^3 + \frac{1}{2}t_-^2 t_+, \tag{C8}$$

yields

$$I = \frac{1}{2\pi^2} \int_{-\infty}^{\infty} \mathrm{d}t_- \frac{\sin\left[(2p + t_-)a\right]}{2p + t_-} \times \int_{-\infty}^{\infty} \mathrm{d}t_+ \exp\left\{i\left[\frac{1}{3}2t_+^3 + \left(\frac{1}{2}t_-^2 + 2\zeta\right)t_+\right]\right\}. \tag{C9}$$

Finally, we carry out the integration over t_+ by recalling the integral representation, Eq. (C3), of the Airy function together with the substitution $t \equiv 2^{1/3}t_+$, and with $u \equiv 2^{-2/3}t_-$, we arrive at the expression

$$I = \frac{2^{1/3}}{\pi} \int_{-\infty}^{\infty} \mathrm{d}u \, \mathrm{Ai}\left[u^2 + 2^{2/3}\zeta\right] \frac{\sin\left[(2p + 2^{2/3}u)a\right]}{2p + 2^{2/3}u}. \tag{C10}$$

When we substitute this representation of I into the formula, Eq. (C1), for the Wigner function W_n, we find

$$W_n(z,k) = \Theta(z)\, 2^{1/3} \frac{N_n^2}{\pi^2} \int_{-\infty}^{\infty} \mathrm{d}u \, \mathrm{Ai}[u^2 + 2^{2/3}(\kappa z - \epsilon_n)] \times \frac{\sin\left[(2k + 2^{2/3}u\kappa)z\right]}{2k + 2^{2/3}u\kappa} \tag{C11}$$

or

$$W_n(z,k) = \Theta(z)\, \mathcal{N}_n \int_{-\infty}^{\infty} \mathrm{d}u \, \mathcal{A}(z,u)\mathcal{D}(2z, k + 2^{-1/3}u\kappa), \tag{C12}$$

where we have recalled the definition, Eq. (A10), of the diffraction kernel $\mathcal{D}$ and have introduced the abbreviations

$$\mathcal{N}_n \equiv 2^{-2/3}\frac{N_n^2}{\pi} \tag{C13}$$

and

$$\mathcal{A}(z;u) \equiv \mathrm{Ai}[u^2 + d_n(z)] \tag{C14}$$

with the displacement

$$d_n(z) \equiv 2^{2/3}(\kappa z - \epsilon_n). \tag{C15}$$

To gain deeper insight into the qualitative behavior of the function, it is instructive to split the remaining integration over u into its negative and positive domain,

$$W_n(z,k) = \Theta(z)\, \mathcal{N}_n \int_0^{\infty} \mathrm{d}u \, \mathcal{A}(z;u)\left[\mathcal{D}_+(z,k;u) + \mathcal{D}_-(z,k;u)\right], \tag{C16}$$

with

$$\mathcal{D}_\pm(z,k;u) = \mathcal{D}(2z, k \pm 2^{-1/3}u\kappa). \tag{C17}$$

In this representation, the symmetry, Eq. (6), with respect to the coordinate axis is apparent.

We conclude this analysis of the Wigner integral, Eq. (C2), for the *q*Bounce wave function by noting that the method of the stationary phase[16] when applied to Eq. (C9) may yield deeper insight into the form of the Wigner function. However, we postpone this approach to a future publication.

2. Qualitative behavior

Now, we are in the position to study characteristic features of the Wigner function W_n corresponding to the *q*Bounce wave function ψ_n based on the integral representation, Eq. (C16). For the sake of simplicity, we first restrict our analysis to the ground state corresponding to $n = 1$. We conclude by briefly discussing the general case.

We start by identifying the origin of the ripples in the Wigner function exemplified on the top of Fig. 4 as a function of k for $z = 1$. For this purpose, we first note that the integration in Eq. (C16) runs over positive values of u only, and the integrand consists of the product of the shifted Airy function $\mathcal{A} = \mathcal{A}(z; u)$ and the two diffraction kernels $\mathcal{D}_\pm(z, k; u)$, given by Eq. (C17).

For a fixed z, the Airy function defining $\mathcal{A}$ is shifted to the right by the amount $d_1(z)$ creating a maximum along the positive u axis as shown by the orange curves in Fig. 4. For values of u beyond this maximum, we observe the characteristic exponential decay of the Airy function. Hence, it is the extension of the Airy function in u that determines the region of integration.

Next, we address the influence of $\mathcal{D}$, shown in Fig. 4 by the green curves, on the integration. For a fixed wave vector k, the two components $\mathcal{D}_\pm$ of the diffraction kernel $\mathcal{D}$ have a maximum at $u = \mp 2^{1/3} k/\kappa$ with decaying oscillations on both sides.

Hence, for increasing values of k displayed in Fig. 4 indicated on the top curve by arrows, the two dominant maxima of $\mathcal{D}_-$ and $\mathcal{D}_+$ shift to the right and left, respectively. Since the integration is restricted to the positive domain only, the main contribution of $\mathcal{D}$ to the integral arises from the component $\mathcal{D}_-$ corresponding to a shift to the right.

We can now understand the appearance of the ripples depicted on the top of Fig. 4. Indeed, the integrand of the Wigner function, shown in Fig. 4 by the blue lines, consists of the shifted Airy function $\mathcal{A}$, which is independent of k, and the diffraction kernel $\mathcal{D}$ moving to the right along the u axis with increasing k. The peaks and valleys of $\mathcal{D}_-$ move through the integration region resulting in an integrand with either mainly positive (a) and (d) or negative (b) values, or as many positive as negative contributions (d) as shown in the individual panels of Fig. 4. Hence, the Wigner function displays oscillations along the k axis.

Next, we address the behavior of the Wigner function for a fixed k and growing values of z as exemplified on the top of Fig. 5. In this case, the dependence of $\mathcal{A}$ on z becomes important. Indeed, due to the position dependence of the displacement d_1, Eq. (C15), the Airy function, along with its exponential tail, experiences a shift to the left as demonstrated in Fig. 5 for four values of z marked again on the top curve by arrows. Therefore, the region of integration gets reduced, and we expect to see an exponential decay along the z axis in the Wigner function.

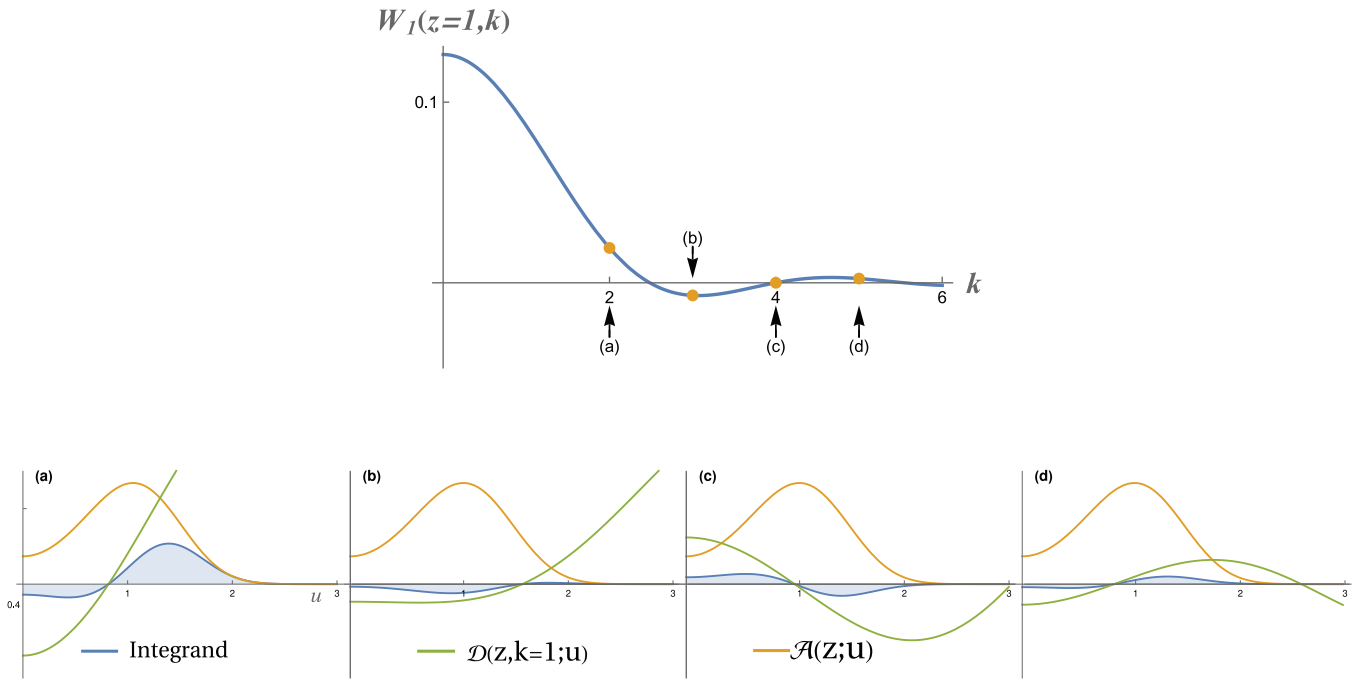

FIG. 4. Origin of the ripples in the Wigner function W_1 corresponding to the *q*Bounce ground state wave function ψ_1, explained by the integral representation, Eq. (C16). On the top, we depict W_1 as a function of k for $z = 1$. Below, we show for four different characteristic values (a)–(d) of k indicated on the top curve by arrows, the shifted Airy function $\mathcal{A} = \mathcal{A}(z; u)$ (orange line), the integration kernel $\mathcal{D} = [\mathcal{D}_+(z, k; u) + \mathcal{D}_-(z, k; u)]$ (green line), and the integrand (blue line), given by their product, as a function of the integration variable u. The axes in the four pictures are identical. For increasing k, $\mathcal{D}$ with its oscillatory wings moves to the right, and as a result, the integral oscillates as well, in complete agreement with the top curve.

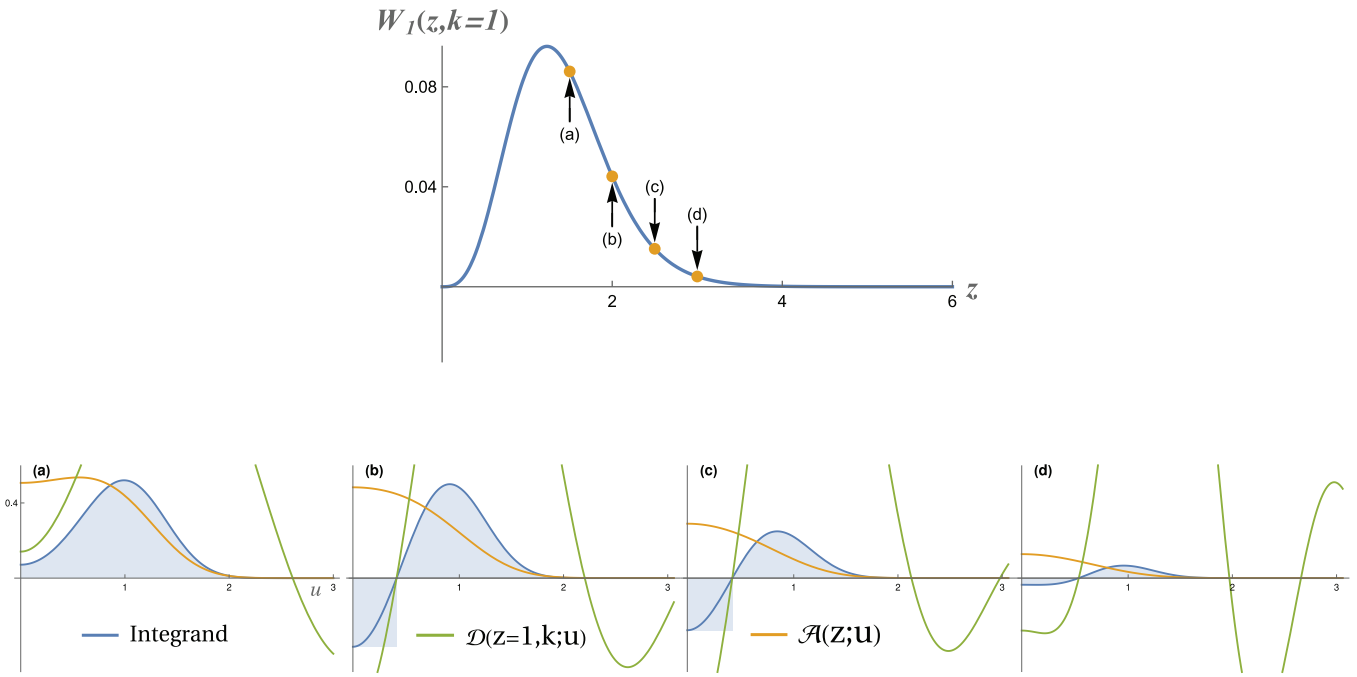

FIG. 5. Origin of the exponential decay (top) of the Wigner function W_1 corresponding to the *q*Bounce ground state wave function ψ_1 for fixed $k = 1$ but increasing z using the integral representation, Eq. (C16). On the top, we depict W_1 as a function of z for $k = 1$, and below, we show for four different characteristic values (a)–(d) of z, indicated on the top curve by arrows, the shifted Airy function $\mathcal{A} = \mathcal{A}(z; u)$ (orange line), the diffraction kernel $\mathcal{D} = [\mathcal{D}_+(z, k; u) + \mathcal{D}_-(z, k; u)]$ (green line), and the integrand (blue line), given by their product, as a function of the integration variable u. The axes in the four pictures are identical. Due to the motion of the decaying part of $\mathcal{A}$ to the left, the integral and, thus, the Wigner function W_1 decay.

For excited states, that is, $n > 1$, the shift $d_n(z)$ of $\mathcal{A}$ increases with n. Depending on the coordinate z, $\mathcal{A}$ now has up to n maxima inside the positive domain. Hence, the integration interval gets enlarged, but the overall behavior of the functions involved does not change. Therefore, we still expect the Wigner function to display oscillations along the k axis and an exponential decay along the z axis. For a pictorial representation of W_n for $n > 1$, we refer to Ref. 37.

3. Diffraction integral

We conclude this appendix by verifying that W_n in the form of Eq. (C12) satisfies the diffraction integral, Eq. (A14). Here, we apply the convolution identity Eq. (A15).

From Eq. (C12), we find for the right-hand side of Eq. (A14) the expression

$$RS = \Theta^2 \mathcal{N}_n \int_{-\infty}^{\infty} \mathrm{d}u\, \mathcal{A}(z; u)\mathcal{J}(u), \tag{C18}$$

where we have interchanged the order of integrations and introduced the abbreviation

$$\mathcal{J}(u) \equiv \int_{-\infty}^{\infty} \mathrm{d}k'\, \mathcal{D}(a, k' + 2^{-1/3}u\kappa)\mathcal{D}(a, k + k'), \tag{C19}$$

with $a = 2z$.

With the help of the convolution identity, Eq. (A15), we immediately arrive at

$$\mathcal{J}(u) = \mathcal{D}(a, k - 2^{-1/3}u\kappa), \tag{C20}$$

which with the help of the relation, Eq. (A1), reduces to

$$RS = W_n, \tag{C21}$$

where in the last step, we have introduced the integration variable $u' \equiv -u$ and recalled the expression, Eq. (C12), of W_n.

APPENDIX D: TIME-EVOLVED WAVE FUNCTIONS

In this Appendix, we derive expressions for the free time evolution of the three model wave functions, ψ_c, ψ_e, and ψ_k, determined by Eqs. (10), (19), and (24), respectively. Throughout this Appendix, we use the propagator, Eq. (30), of a free particle.

In the three examples, the time-evolved wave functions follow from the integral

$$\mathcal{I}(z, t; \beta) \equiv N_p(t) \int_0^{\infty} \mathrm{d}z_0\, \mathrm{e}^{i\alpha(t)(z-z_0)^2} \mathrm{e}^{-\beta z_0}, \tag{D1}$$

where $N_p = N_p(t)$ and $\alpha = \alpha(t)$ are given by Eqs. (31) and (32), respectively.

Indeed, we find immediately

$$\psi_c(z,t) = \mathcal{I}(z,t;\beta=0) \tag{D2}$$

and

$$\psi_e(z,t) = N_e\mathcal{I}(z,t;\beta) \tag{D3}$$

together with

$$\psi_k(z,t) = -N_k\frac{\partial}{\partial\beta}\mathcal{I}(z,t;\beta). \tag{D4}$$

When we complete the square, the integral $\mathcal{I}$, defined by Eq. (D1), takes the form

$$\mathcal{I} = N_p e^{-\beta z} e^{\frac{i\beta^2}{4\alpha}} \int_0^\infty \mathrm{d}z_0\, e^{i\alpha\left(z-z_0+\frac{\beta}{2i\alpha}\right)^2}, \tag{D5}$$

which with the substitution $-t^2 \equiv i\alpha(z - z_0 + \frac{\beta}{2i\alpha})^2$ leads us to the result

$$\mathcal{I} = \frac{1}{2}e^{-\beta z}e^{i\frac{\beta^2}{4\alpha}}\,\mathrm{erfc}(b), \tag{D6}$$

with

$$b(z,t) \equiv -\sqrt{\frac{\alpha(t)}{i}}\left[z+\frac{\beta}{2i\alpha(t)}\right]. \tag{D7}$$

Here, we have recalled the definition, Eq. (31), of the normalization factor N_p of the propagator, as well as the definition[40]

$$\mathrm{erfc}(z) \equiv \frac{2}{\sqrt{\pi}}\int_z^\infty \mathrm{d}t\, e^{-t^2} \tag{D8}$$

of the complementary error function.

From the expression, Eq. (D6), for the integral $\mathcal{I}$ and the definition, Eq. (D7), of b, we find from Eq. (D2) the result

$$\psi_c(z,t) = \frac{1}{2}\mathrm{erfc}\left(-\sqrt{\frac{\alpha(t)}{i}}z\right). \tag{D9}$$

When we substitute the expression, Eq. (D6), into the formula, Eq. (D3), we arrive at

$$\psi_e(z,t) \equiv \sqrt{\frac{\beta}{2}}e^{-\beta z}e^{\frac{i\beta^2}{4\alpha(t)}}\,\mathrm{erfc}\left[b(z,t)\right]. \tag{D10}$$

Here, we have also used the definition, Eq. (18), of N_e.

In order to find the time evolution of the modified exponential function given by Eq. (D4), we need to differentiate the integral $\mathcal{I}$, Eq. (D6), with respect to β, leading us to the expression

$$\frac{\partial\mathcal{I}}{\partial\beta} = \frac{1}{2}e^{-\beta z}e^{\frac{i\beta^2}{4\alpha}}\left\{\mathrm{erfc}\,(b)\left[-z+\frac{i\beta}{2\alpha}\right]+\frac{\partial}{\partial\beta}\mathrm{erfc}(b)\right\}. \tag{D11}$$

From the definition, Eq. (D8), of the complementary error function, we find

$$\frac{\mathrm{d}}{\mathrm{d}z}\mathrm{erfc}(z) = -\frac{2}{\sqrt{\pi}}e^{-z^2}, \tag{D12}$$

and thus,

$$\frac{\partial}{\partial\beta}\mathrm{erfc}(b) = \frac{1}{\sqrt{\pi\alpha}}\mathrm{e}^{-b^2}\mathrm{e}^{-i\frac{3\pi}{4}}. \tag{D13}$$

Hence, the time-evolved modified exponential wave function reads

$$\psi_k = -\frac{N_k}{2}e^{-\beta z}e^{\frac{i\beta^2}{4\alpha}}\left\{-\mathrm{erfc}\,(b)\left[z+\frac{\beta}{2i\alpha}\right]+\frac{1}{\sqrt{\pi\alpha}}e^{-b^2}e^{-i\frac{3\pi}{4}}\right\}. \tag{D14}$$

The definition, Eq. (D7), of b allows us to simplify this expression and arrive at

$$\psi_k(z,t) = -\frac{N_k}{2}e^{-\beta z}e^{\frac{i\beta^2}{4\alpha}}\sqrt{\frac{1}{\alpha}}\mathrm{e}^{i\frac{\pi}{4}}\left[\mathrm{erfc}(b)b-\frac{e^{-b^2}}{\sqrt{\pi}}\right]. \tag{D15}$$

Hence, the probability density $|\psi_k|^2$ is then given by

$$|\psi_k(z,t)|^2 = \frac{N_k^2}{4\alpha}\,\mathrm{e}^{-2\beta z}\left\{|\mathrm{erfc}\,(b)\,b|^2+\frac{\mathrm{e}^{2\beta z}}{\pi}-\frac{2}{\sqrt{\pi}}\,\mathrm{Re}\left[\mathrm{erfc}(b^*)\,b^*\mathrm{e}^{-b^2}\right]\right\}, \tag{D16}$$

where the asterisk denotes the complex conjugate.

APPENDIX E: TIME-EVOLVED *q*BOUNCE WAVE FUNCTION

In this Appendix, we cast the integral, Eq. (34), for the free time evolution of the *q*Bounce wave function φ_n, given by Eq. (26), into a form, which allows its numerical evaluation.

The free time evolution is determined by the integral

$$I_n(z,t) \equiv N_p(t)N_n\int_0^\infty \mathrm{d}z_0\,\mathrm{e}^{i\alpha(t)(z-z_0)^2}\,\mathrm{Ai}(\kappa z_0-\epsilon_n), \tag{E1}$$

and when we recall the definition, Eq. (C3), of the Airy function, we find

$$I_n = \frac{N_pN_n}{2\pi}\int_0^\infty \mathrm{d}z_0\int_{-\infty}^\infty \mathrm{d}y\,\mathrm{e}^{i\alpha(z-z_0)^2}\mathrm{e}^{i\left[\frac{1}{3}y^3+(\kappa z_0-\epsilon_n)y\right]}. \tag{E2}$$

Completing the square and using the substitution $-r^2 \equiv i\alpha(z_0 + \kappa y/2\alpha - z)^2$, we get

$$I_n = \frac{N_pN_n}{2\pi}\sqrt{\frac{i}{\alpha}}\int_{-\infty}^\infty dy\int_{r_0(y;z)}^\infty \mathrm{d}r\,\mathrm{e}^{-r^2}\,\mathrm{e}^{i\left[\frac{1}{3}y^3-\frac{\kappa^2}{4\alpha}y^2+(\kappa z-\epsilon_n)y\right]}, \tag{E3}$$

with $r_0(y;z) \equiv \sqrt{\frac{\alpha}{i}\left(\frac{\kappa y}{2\alpha}-z\right)}$.

With the definition Eq. (D8) of the complementary error function and the definition, Eq. (31), of N_p, we finally arrive at

$$I_n = \frac{N_n}{4\pi}\int_{-\infty}^\infty \mathrm{d}y\,\mathrm{erfc}\left[\sqrt{\frac{\alpha}{i}}\left(\frac{\kappa y}{2\alpha}-z\right)\right]\mathrm{e}^{i\left[\frac{1}{3}y^3-\frac{\kappa^2}{4\alpha}y^2+(\kappa z-\epsilon_n)y\right]}, \tag{E4}$$

which allows us a numerical evaluation.

REFERENCES

[1] M. Born and P. Jordan, *Elementare Quantenmechanik* (Springer, Berlin, 1930).
[2] E. Schrödinger, *Collected Papers on Wave Mechanics* (AMS Chelsea Publishing, 1982).
[3] R. P. Feynman, "Space-time approach to non-relativistic quantum mechanics," Rev. Mod. Phys. **20**, 367–387 (1948).

[4]E. Wigner, "On the quantum correction for thermodynamic equilibrium," Phys. Rev. **40**, 749–759 (1932).
[5]D. Bohm, *Quantum Theory* (Prentice Hall, Englewood Cliffs, NJ, 1951).
[6]G. Herzberg, *Molecular Spectra and Molecular Structure. I. Spectra of Diatomic Molecules* (Van Nostrand, Princeton, NJ, 1965).
[7]D. L. Hill and J. A. Wheeler, "Nuclear constitution and the interpretation of fission phenomena," Phys. Rev. **89**, 1102–1145 (1953).
[8]W. Schleich and J. A. Wheeler, "Oscillations in photon distributions of squeezed states and interference in phase space," Nature **326**, 574–577 (1987).
[9]J. A. C. Gallas, W. P. Schleich, and J. A. Wheeler, "Waves at walls, corners, heights: Looking for simplicity," Appl. Phys. B **60**, 279–287 (1995).
[10]J. Bestle, W. P. Schleich, and J. A. Wheeler, "Anti-stealth: WKB grapples with a corner," Appl. Phys. B **60**, 289–299 (1995).
[11]G. Sweetman, *Stealth Bomber: Invisible Warplane, Black Budget* (Motorbooks, Osceola, WI, 1989).
[12]A. Mitra, "Quantum quench dynamics," Annu. Rev. Condens. Matter Phys. **9**, 245–259 (2018).
[13]K. Schönhammer, "Quantum versus classical quenches and the broadening of wave packets," Am. J. Phys. **92**, 466–472 (2024).
[14]M. Born and E. Wolf, *Principles of Optics* (Pergamon Press, 1964).
[15]M. Hillary, R. F. O'Connell, M. O. Scully, and E. P. Wigner, "Distribution functions in physics: Fundamentals," Phys. Rep. **106**, 121–167 (1984).
[16]W. P. Schleich, *Quantum Optics in Phase Space* (Wiley-VCH, 2001).
[17]D. Goodings and T. Szeredi, "The quantum bouncer by the path integral method," Am. J. Phys. **59**, 924–930 (1991).
[18]H. Abele, G. Cronenberg, P. Geltenbort, T. Jenke, T. Lins, and H. Saul, "qBounce, the quantum bouncing ball experiment," Phys. Procedia **17**, 4–9 (2011).
[19]T. Jenke, P. Geltenbort, H. Lemmel, and H. Abele, "Realization of a gravity-resonance-spectroscopy technique," Nat. Phys. **7**, 468–472 (2011).
[20]H. Abele, "Caustics and the free fall," in *Talk at the Conference: From GHZ to Tic Tac Toe: A Symposium to Celebrate Danny Greenberger's 90th Birthday, 27 September 2024* (Vienna University, 2024).
[21]P. Stifter, C. Leichtle, W. P. Schleich, and J. Marklof, "Das Teilchen im Kasten: Strukturen in der Wahrscheinlichkeitsdichte," Z. Naturforsch. **52**, 377–385 (1997).
[22]F. Grossmann, J. M. Rost, and W. P. Schleich, "Spacetime structures in simple quantum systems," J. Phys. A: Math. Gen. **30**, L277–L283 (1997).
[23]M. Berry, I. Marzoli, and W. P. Schleich, "Quantum carpets, carpets of light," Phys. World **14**, 39–46 (2001).
[24]L. Cohen, "Wigner distribution for finite duration or band-limited signals and limiting cases," IEEE Trans. Acoust., Speech, Signal Process. **35**, 796–806 (1987).
[25]J. P. Dahl and M. Springborg, "The Morse oscillator in position space, momentum space, and phase space," J. Chem. Phys. **88**, 4535–4547 (1988).
[26]M. Hug, C. Menke, and W. P. Schleich, "How to calculate the Wigner function from phase space," J. Phys. A: Math. Gen. **31**, L217–L224 (1998).
[27]J. P. Dahl and M. Springborg, "Wigner's phase space function and atomic structure: I. The hydrogen atom ground state," Mol. Phys. **47**, 1001–1019 (1982).
[28]M. Springborg and J. P. Dahl, "Wigner's phase-space function and atomic structure: II. Ground states for closed-shell atoms," Phys. Rev. A **36**, 1050 (1987).
[29]J. P. Dahl, "On the oscillatory decay of atomic Wigner functions," Phys. Chem. **99**, 2727–2731 (1995).
[30]M. V. Berry, "Fringes decorating anticaustics in ergodic wavefunctions," Proc. R. Soc. Lond. A **424**, 279–288 (1989), see https://www.jstor.org/stable/2398369.
[31]A. M. O. De Almeida, "The Weyl representation in classical and quantum mechanics," Phys. Rep. **295**, 265–342 (1998).
[32]G. Süssmann, *Einführung in die Quantenmechanik* (Bibliographisches Institut, 1963).
[33]A. Das and A. C. Melissinos, *Quantum Mechanics: A Modern Introduction* (CRC Press, 1986).
[34]A. Steane, P. Szriftgiser, P. Desbiolles, and J. Dalibard, "Phase modulation of atomic de Broglie waves," Phys. Rev. Lett. **74**, 4972–4975 (1995).
[35]P. Szriftgiser, D. Guéry-Odelin, M. Arndt, and J. Dalibard, "Atomic wave diffraction and interference using temporal slits," Phys. Rev. Lett. **77**, 4–7 (1996).
[36]V. V. Nesvizhevsky, H. G. Börner, A. K. Petukhov, H. Abele, S. Baeßler, F. J. Rueß, T. Stöferle, A. Westphal, A. M. Gagarski, G. A. Petrov, and A. V. Strelkov, "Quantum states of neutrons in the earth's gravitational field," Nature **415**, 297–299 (2002).
[37]M. Suda, M. Faber, J. Bosina, T. Jenke, C. Käding, J. Micko, M. Pitschmann, and H. Abele, "Spectra of neutron wave functions in Earth's gravitational field," Z. Naturforsch. A **77**, 875–898 (2022).
[38]E. Kajari, N. L. Harshman, E. M. Rasel, S. Stenholm, G. Süßmann, and W. P. Schleich, "Inertial and gravitational mass in quantum mechanics," Appl. Phys. B **100**, 43–60 (2010).
[39]O. Vallée and M. Soares, *Airy Functions and Applications to Physics* (Imperial College Press, 2010).
[40]M. Abramowitz and I. A. Stegun, *Handbook of Mathematical Functions with Formulas, Graphs, and Mathematical Tables* (Dover, 1964).
[41]M. R. Gonçalves, W. B. Case, A. Arie, and W. P. Schleich, "Single-slit focusing and its representations," Appl. Phys. B **123**, 121 (2017).
[42]F. Stenger, "Numerical methods based on Whittaker cardinal, or sinc functions," SIAM Rev. **23**, 165–224 (1981).